



## MEGA-EARTHQUAKES RUPTURE SCENARIOS AND STRONG MOTION SIMULATIONS FOR LIMA, PERU

Nelson PULIDO<sup>1</sup>, Hernando TAVERA<sup>2</sup>, Zenón AGUILAR<sup>3</sup>, Diana CALDERÓN<sup>4</sup>, Mohamed CHLIEH<sup>5</sup>, Toru SEKIGUCHI<sup>6</sup>, Shoichi NAKAI<sup>7</sup>, and Fumio YAMAZAKI<sup>7</sup>

### SUMMARY

The recent 2011 Tohoku-oki earthquake occurred in a region where giant megathrust earthquakes were not expected. This earthquake proved the difficulty to assess seismic hazard mainly based on information from historical earthquakes. In this study we propose a methodology to estimate the slip distribution of megathrust earthquakes based on a model of interseismic coupling (ISC) distribution in subduction margins as well as information of historical earthquakes, and apply the method to the Central Andes region in Peru. The slip model obtained from geodetic data represents the large scale features of asperities within the megathrust, which is appropriate for simulation of long period waves and tsunami modelling. For the simulation of a broadband strong ground motion it becomes necessary to introduce small scale heterogeneities to the source slip to be able to simulate high frequency ground motions. To achieve this purpose we propose “broadband” source models constructed by adding the slip model inferred from the geodetic data, and short wavelength slip distributions obtained from a Von Karman PSD function with random phases. Using these slip models and assuming several hypocenter locations we calculate a set of strong ground motions within Lima and incorporate site effects obtained from microtremors array surveys.

### INTRODUCTION

Recent mega-earthquakes in Sumatra (2004), Chile (2010) and Japan (2011) have highlighted the enormous hazard associated with these giant subduction events. In particular the 2011 Tohoku-oki earthquake proved the difficulty to assess seismic hazard mainly based on information from historical earthquakes. Due to the limited span of earthquake catalogues, other source of information such as geological or geodetic data might be considered for hazard assessment of future mega-earthquakes.

1 Researcher, National Research Institute for Earth Science and Disaster Prevention, Japan. Email: nelson@bosai.go.jp

2 Researcher, Instituto Geofísico del Perú, Peru. Email: hernando.tavera@igp.gob.pe

3 Professor, Universidad Nacional de Ingeniería, Perú. Email: zaguilard@zergeosystemperu.com

4 Assistant Professor, Universidad Nacional de Ingeniería, Perú. Email: dianalucc@gmail.com

5 Professor, University Nice-Sophia, France. Email: chlieh@geoazur.unice.fr

6 Assistant Professor, Chiba University, Japan. Email: tsekiguchi@faculty.chiba-u.jp

7 Professor, Chiba University, Japan. Email: nakai@faculty.chiba-u.jp

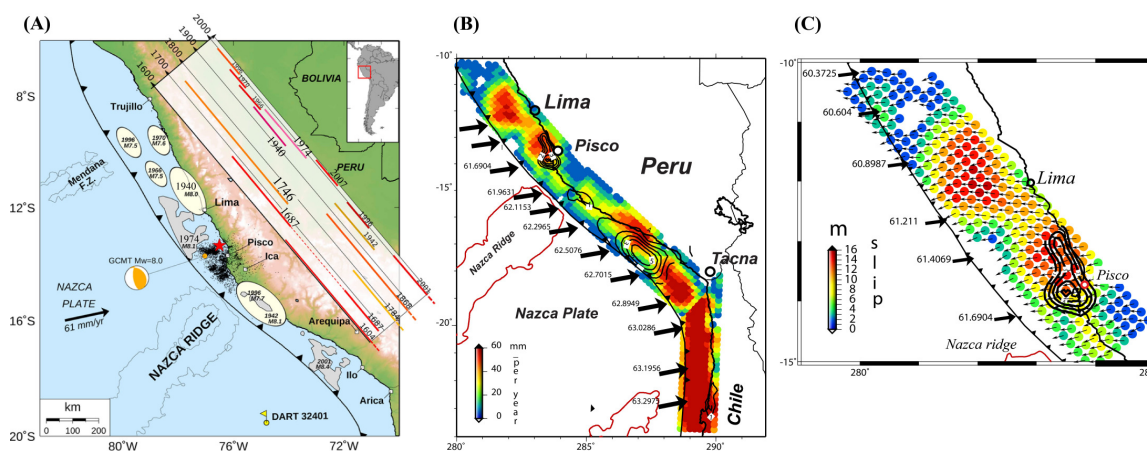


Fig. 1. A) Historical earthquakes along the Nazca subduction zone in Peru (Sladen et al. 2010). B) Slip deficit rate model in Peru and northern Chile obtained from geodetic measurements (Chlieh et al. 2010). C) Slip distribution of a scenario earthquake for the subduction zone off-Lima, obtained by combining the slip deficit rate in (B) with an interseismic period of 265 years since the 1746 earthquake. The slip contours of the 2007 Pisco earthquake are displayed in figures B and C.

In recent years the development of GPS and SAR interferometry is making possible to measure the strain build up associated with plate convergence in many earthquake prone regions around the world (Chlieh et al., 2008, and Perfettini et al. 2010). Recent studies have suggested that subducting plates are either locked or creeping aseismically, and that a patchwork of locked or coupled regions during the interseismic period may be related with asperities of earthquakes (Moreno et al. 2010). In this study we propose a methodology for seismic hazard estimation of megathrust earthquakes based on a model of interseismic coupling (ISC) distribution of subduction zones as well as information of historical earthquakes, and apply the method to the Central Andes region in Peru. Central Peru, North of the Nazca ridge, has been repeatedly affected by large earthquakes such as the 28 October 1746 which is reportedly the worst earthquake Lima has experienced since its foundation. Intensity reports as well as a tsunami record suggest a moment magnitude of  $\sim 8.8$  for this earthquake (Dorbath et al. 1990). The 1746 earthquake was followed by a long period of quiescence until a sequence of magnitude 7-8 earthquakes in the 20<sup>th</sup> century starting with the 1940 earthquake up to the M8.1 Pisco earthquake in 2007 (Sladen et al., 2010) (Figure 1A). We use this information combined with an interseismic coupling model of Central Andes to elaborate a scenario for a megathrust earthquake that could likely affect the Lima metropolitan region.

## SCENARIO EARTHQUAKES

### *Interseismic coupling (ISC) and scenario earthquake*

A model of interseismic coupling (ISC for Central Andes (Chlieh) indicates the existence of two strongly coupled regions, the first one off-shore Lima and the second one off-shore Pisco city (Figure 1B). Assuming an interseismic period of 265 years since the last megathrust earthquake that stroke Central Andes in 1746, up to 2010, we obtained a slip deficit equivalent to an earthquake with a moment magnitude of 8.9 (Figure 1C).

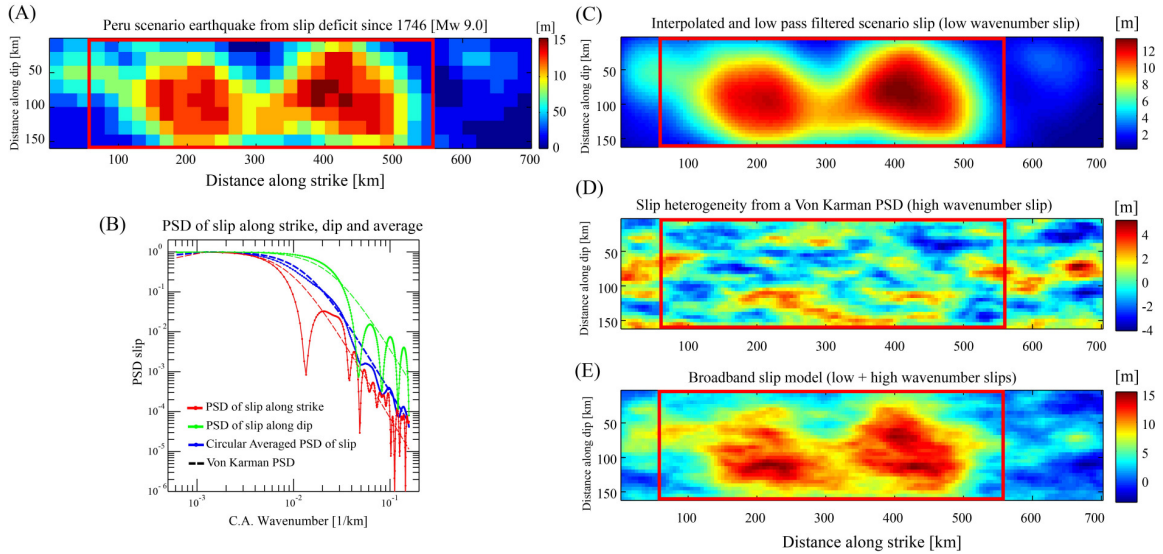


Fig. 2 A) Slip distribution of the Central Andes scenario earthquake from ISC model. B) PSD of slip along strike (red), dip (green) and circular average (blue). Dashed lines correspond to the best fit Von Karman PSD function to the PSD of slip. C) Interpolated (to a 5 km grid spacing) and low-pass wavenumber filtered slip in A). D) Short wavelength slip obtained from the Von Karman PSD function of slip in B) and a random phase. E) Broadband slip obtained by adding low and high wave number slips in C and D. Red boxes indicate the assumed source area for the slip scenarios.

### Broadband slip scenario earthquake

The geodetic slip model (GSM) obtained from the ISC, has a maximum slip of approximately 15 m, the source dimensions are approximately 500 km along strike and 160 km along dip, and the grid spacing is 20 km (Figure 2A). The moment magnitude, calculated using a rigidity of 39GPa is 8.9. The GSM is characterized by a smooth distribution of asperities (Figure 2A). This model is appropriate for the simulation of long period seismic waves as well as for tsunami modelling despite the large grid spacing employed. However for the simulation of a broadband strong ground motion it becomes necessary to introduce small scale complexities to the source slip to be able to simulate high frequency ground motions. To achieve this purpose we propose a “broadband” source model in which large scale features of the model are constructed from the GSM, and the short wavelength slip distribution is obtained from spatially correlated random noise. To obtain the parameters of this short wavelength slip we first calculate the power spectrum density (PSD) of our GSM, along the strike and dip directions (red and green lines in Fig.2B), as well as for a circular average (blue line in Fig.2B), and then fit a Von Karman PSD function to the observed spectra,

$$P(k_s, k_d) = \frac{k_s k_d}{[1 + a_s^2 k_s^2 + a_d^2 k_d^2]^{H+1}} \quad (1)$$

where  $k_s$  and  $k_d$  are wavenumbers along strike and dip,  $a_s$  and  $a_d$  are the autocorrelation distances along strike and dip, and  $H$  is the Hurst exponent defining the spectral decay. Our fit to the PSD of the GSM yielded values of  $110 \text{ km}^{-1}$ ,  $40 \text{ km}^{-1}$ , and 1 for  $a_s$ ,  $a_d$  and  $H$  respectively (dashed lines in Figure 2B). To calculate a “broadband” slip we first interpolate the original GSM to a smaller grid

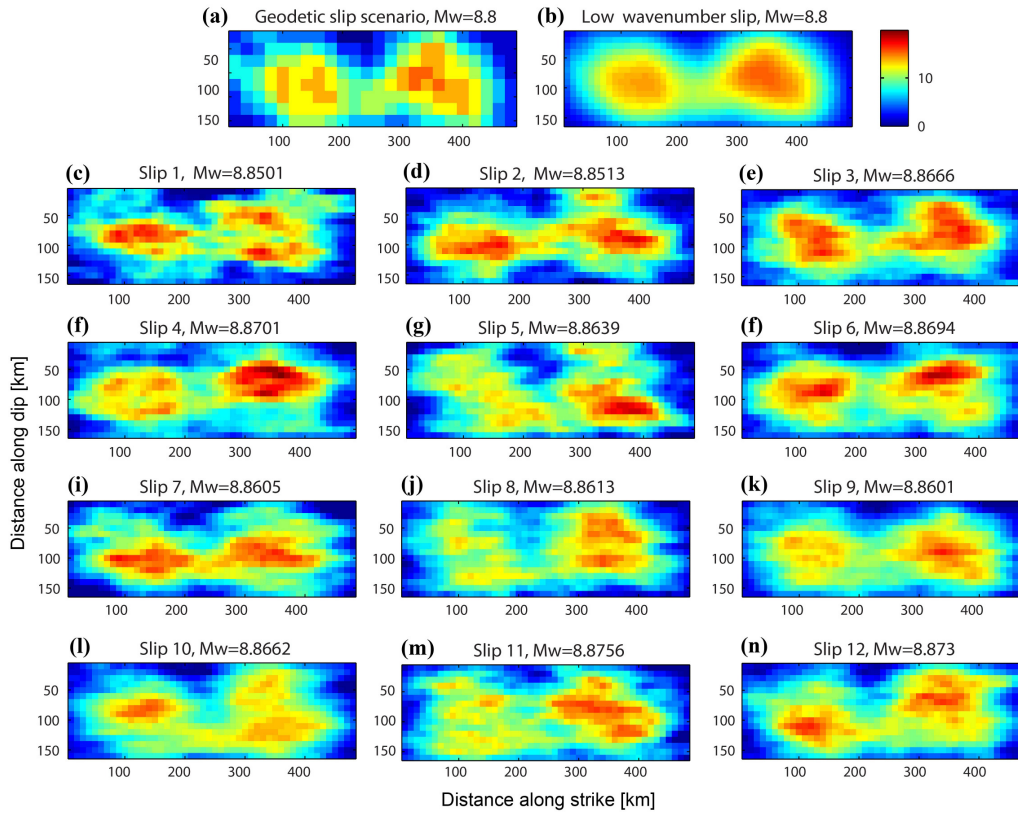


Fig. 3 a) Slip scenario obtained from ISC model. b) Interpolated and low-pass wavenumber filtered slip model in a). c) to n) Broadband slip scenarios for 12 random realizations of short wavelength slip.

interval, and apply a low-pass filter for wavenumbers smaller than a crossover wavenumber ( $k_{\text{cross}}$ ) equal to 0.05, to get a long wavelength slip distribution (Figure 2C). Then we generate a correlated random slip model by using the aforementioned Von Karman PSD function (eq. No.1), and a random phase. We then apply a high-pass filter to this correlated random slip model for wavenumbers higher than  $k_{\text{cross}}$ , to get the short wavelength slip (Figure 2D). Finally we add the long and short wavelength slips to obtain a broadband wavelength slip (Figure 2E). The  $k_{\text{cross}}$  value was selected to approximately correspond to the size of the long wavelength asperity (125 km) (Figure 2C), which is about 5 times the corner wavenumber of GSM.

#### Broadband Slip realizations

In order to obtain several broadband slips to be used for the strong motion simulations in Central Andes region, we compute a number of short wavelength slip models realizations. For this purpose we generate 12 sets of normally distributed random numbers with mean 0 and standard deviation 1, for the same source area used for the GSM, calculate their FFT in the wavenumber domain along strike and dip, multiply their spectral amplitude by the square root of the Von Karman PSD function of slip (eq. 1), and get them back to the spatial domain. This procedure is equivalent of assuming a random phase for equation No.1. We finally obtained 12 broadband slip realizations (Figures 3c to 3n) by adding the long (Fig. 3b) and short wavelength slips. For the Central Andes strong motion simulations we have selected a subfault size of 10km.

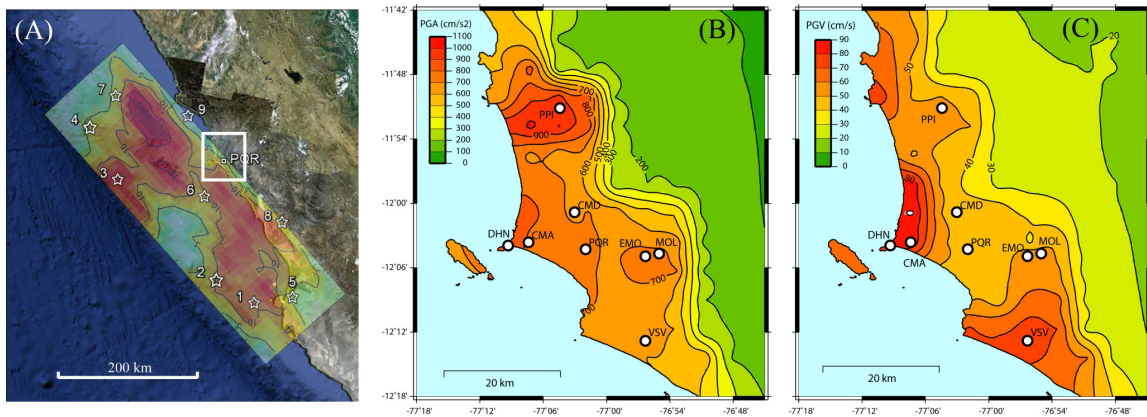


Fig. 4 A) Scenario slip No.5 (Fig. 3g) and all assumed hypocenter locations for the rupture scenarios (stars). The simulation region in Lima is indicated by a white rectangle. B) Average of simulated PGA distributions in Lima for slip No.5 and all assumed hypocenters in A). C) Same as A) but for the simulated PGV.

## STRONG MOTION SIMULATIONS

### *Strong motion simulation method*

To perform the strong motion simulations we follow the hybrid method of Pulido and Kubo (2004). This procedure combines a deterministic simulation at low frequencies (0.01–1 Hz) with a semi-stochastic simulation at high frequencies (1–30 Hz). We assume a finite fault earthquake source embedded in a flat-layered 1D velocity structure. In Pulido and Kubo (2004) the source model was defined as a patchwork of rectangle asperities embedded in a finite fault background with constant slip. In this paper we improved this simulation method to be able to handle a general distribution of slip, which is parameterized for a set of uniformly distributed point sources (subfaults). The total ground motion at a given site is obtained by summing the time delayed contributions from all subfaults, by assuming a given rupture velocity and hypocenter location. For the low frequencies, subfault contributions are calculated by using discrete wave number theory (Bouchon, 1981). At high frequencies, the subfault contributions are calculated using a stochastic method that incorporates a frequency dependent radiation pattern. The methodology has been extensively tested and validated through comparison to recorded data in previous studies (i.e. Pulido and Kubo, 2004).

### *Parameters for the strong motion simulation in Lima*

In order to calculate the strong motion simulation for the Lima Metropolitan region we used the 12 broadband slip source models obtained previously. We assumed 9 different locations of starting points of the rupture (Fig. 4A), based on results of Mai et al. (2005), which concluded that earthquakes ruptures tend to nucleate close to regions of large slip. Main parameters for the simulations are the stress drop, moment and rise time distributions across the fault plane, as well as the rupture velocity. We calculated the stress drop distributions for all the broadband slips following Ripperger and Mai. (2004). Rise times of subfaults are assumed to be proportional to the square root of slip. The rupture velocity is assumed to be 72% of the average S-wave velocity at the source, and we added a 5% fluctuation to enhance high frequency radiation. Maximum frequency  $f_{max}$  is set to 10Hz, and we use a  $Q$  value obtained for the Lima region ( $Q=80f^{0.63}$ ) (Quispe, 2011). For the simulation of low frequency waveforms we used a 1D velocity model obtained for the Lima region (Dorbath et al. 1991).

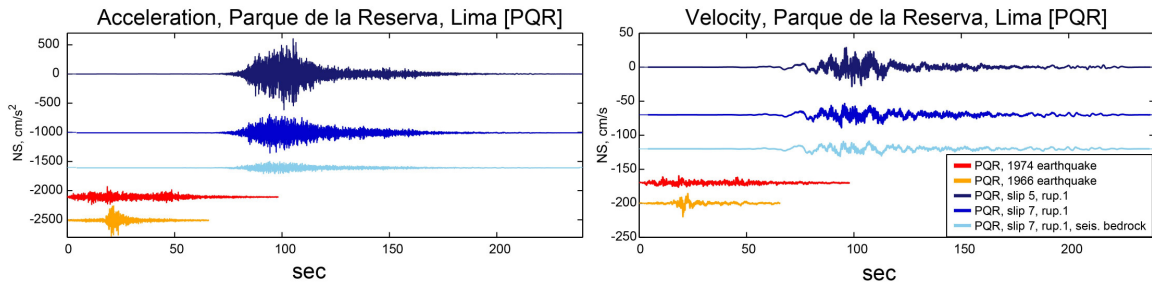


Fig. 5 A) Simulated accelerograms at PQR, for slip No.5 and hypocenter No.1 (dark blue), slip No.7 and hypocenter No.1 (blue), and slip No.7 and hypocenter No.1 for a seismic bedrock soil condition (light blue). The accelerograms in red and orange correspond to records at PQR from the 1974 and 1966 Lima earthquakes. B) Same as in A) but for velocity.

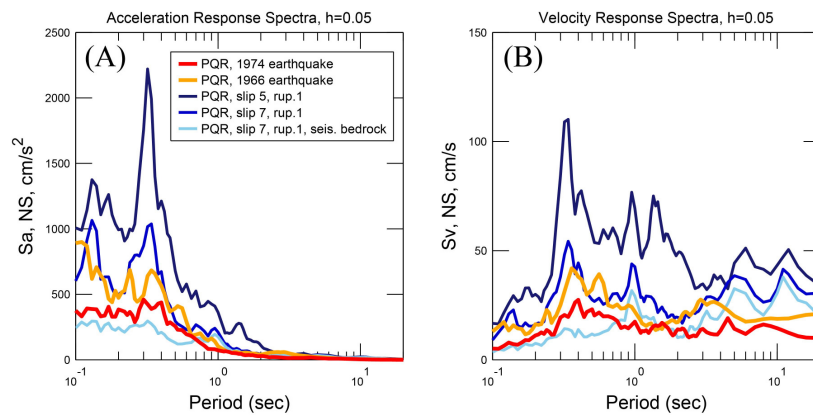


Fig. 6 A) Acceleration response spectra of the simulated NS accelerograms at PQR, for slip No.5 and hypocenter No.1 (dark blue), slip No.7 and hypocenter No.1 (blue), and slip No.7 and hypocenter No.1 for a seismic bedrock soil condition (light blue). The response spectra in red and orange correspond to records at PQR from the 1974 and 1966 Lima earthquakes. B) Same as in A) but for velocity response spectra.

The simulation domain covers all Lima metropolitan region, spanning an area of 50 km by 55 km (white rectangle in Fig. 4A), and a grid spacing of 5 km. We calculated the ew, ns and ud components of broadband frequency strong ground motions at every grid point (140 points) for a seismic bedrock condition ( $V_s=3454$  m/s), for all slip models and assumed hypocenters. This yielded a total of 108 fault rupture scenarios and 45360 synthetic accelerograms. We added site amplifications to all simulations by performing the convolution between the seismic bedrock waveforms with the soil transfer functions at every grid point. Site amplifications were obtained from 8 array microtremors surveys performed at representative geotechnical zones within Lima, which were used to estimate velocity models up to the seismic bedrock condition (Calderón et al., 2012). Soil amplifications at every grid point were estimated by assigning the transfer function values obtained at the closest array measurement point.

#### Strong motion simulation results in Lima

In Figures 4B and 4C we can observe the PGA and PGV distributions for the slip model that yielded the largest ground motion amplitudes among the 12 broadband slip models considered (slip No.5, Fig. 3g), averaged for all assumed rupture starting points scenarios. We can observe that the



largest values of PGA reach  $1000 \text{ cm/s}^2$  at the Puente Piedra district to the North (PPI). Large values of PGA are also observed in the Callao Province ( $900 \text{ cm/s}^2$ ) (DHN, CMA) as well as in La Molina district ( $700 \text{ cm/s}^2$ ) (EMO, MOL). These large values of PGA are closely related with the very large soil amplifications observed at Puente Piedra and Callao for periods around 0.1 to 0.2s, and around 0.1s to 0.7s in La Molina. The PGV distribution on the other hand displays the largest values for Callao ( $80 \text{ cm/s}$ ), followed by large PGV values in Villa El Salvador district ( $70 \text{ cm/s}$ ) (VSV). These large values of PGV are also closely related with the very large soil amplifications observed at Callao for periods around 1s, and at Villa El Salvador for periods around 0.8s to 1.5s (Calderon et al. 2012).

#### *Comparison with records from the 1974 and 1966 earthquakes*

The damaging earthquakes of 1966 (Mw8.0) and 1974 (Mw8.0) that occurred in the subduction zone off-shore Lima (Fig. 1a) were recorded by a strong motion station at Parque de la Reserva (PQR) in central Lima (Fig. 4). At the same location we calculated broadband strong motions for all scenarios, by including site amplifications obtained from results of a microtremor array survey at this site (Calderon et al. 2012). In Figure 5A we may observe several simulated accelerograms at PQR in blue colors, and the observed strong motion records during the 1974 earthquake (red) and 1966 earthquake (orange) for the NS component. In dark blue we display the simulated accelerogram obtained from slip No. 5 and hypocenter No.1. This scenario generates a PGA value comparable to the PGA averaged for all ruptures starts for slip No. 5 (Figure 4B). The waveform in blue corresponds to slip No.7 and hypocenter No.1, which generates a PGA value comparable to the average PGA for all the 108 rupture scenarios considered in this study. The waveform in light blue corresponds to the previous scenario but for a seismic bedrock outcrop condition. We can observe that the PGA amplitudes of the scenarios are about 2~3 times larger than the values observed at PQR during the 1966 and 1974 earthquakes. In Figure 5B we show the time integrated velocity waveforms of accelerograms in Figure 5A. A similar observation can be made from the comparison of PGV amplitudes. We can also observe that the simulated PGV and PGA values for a seismic bedrock outcrop condition (Figure 5A, 5B, light blue), are about 2~3 times smaller than the simulations that incorporate site amplifications (Figure 5A, 5B, blue).

In Figure 6A and 6B we can observe the acceleration and velocity response spectra for all the waveforms detailed in Figure 5. Here we can observe that the spectral amplitudes of the simulated waveforms are as large as 4 times the values observed during the 1974 and 1966 earthquakes at PQR. Another interesting feature is that all the simulated spectra for our scenarios at PQR have a large spectral peak at a period around 0.35s, which is also a clear feature of the observed acceleration and velocity spectra from the 1974 and 1966 earthquakes (Fig. 6A and 6B). These results and the observation of a large amplification at this period in the transfer function at PQR (Calderon et al. 2012), strongly suggest that this large spectral peak is due to site effects. Other interesting feature can be observed at the velocity response spectra for periods longer than 5s. At this range the spectral amplitudes for all scenarios are similar, which may suggest that they might be largely influenced by the source characteristics, as the soil transfer function at PQR above 5s displays no amplification (Calderon et al. 2012)

## CONCLUSIONS.

We have developed a methodology for the estimation of slip scenarios for a future megathrust earthquake originated from the convergence between the Nazca plate and the South American plate. This methodology is based on estimations of interseismic coupling at the megathrust obtained from space geodesy measurements as well as information of historical earthquakes.



Our results show that the Central Andes region in Peru has the potential of generating an earthquake with moment magnitude of 8.9, a peak slip of 15 m and a source area of approximately 500 km along strike and 165 km along dip. We constructed 12 broadband slip source scenarios by adding this long wavelength slip model obtained from geodetic data, with 12 short wavelength slips obtained from a Von Karman PSD function of slip. We calculated the EW, NS and UD components of strong ground motions at Lima for the 12 scenario slips by including 9 possible hypocenter locations for each slip model. Our simulations incorporate site amplifications obtained by microtremors array surveys conducted at the representative geotechnical zones in metropolitan Lima. Our simulation results display values of PGA and PGV as large as  $1000 \text{ cm/s}^2$  and  $80 \text{ cm/s}$  in Lima, for the slip model producing the largest ground motions averaged for all hypocenters locations. Our results indicate that the simulated PGA and PGV in Lima are in average 2~3 times larger than the values observed in PQR, central Lima, during the 1974 and 1966 earthquakes. The observed records and our simulations at PQR indicate a large short period site amplification at 0.35s. Simulated spectral values at PQR at this period are as large as 4 times the values observed during the 1974 and 1966 earthquakes.

#### REFERENCES

1. Calderon, D., T. Sekiguchi, S. Nakai, Z. Aguilar, and F. Lazares, 2012, Study of soil amplification base don microtremor and seismic records in Lima Peru, Jour. Japan Assoc. Earthq. Eng., 12, (2), 1-20.
2. Chlieh, M., H. Perfettini, H. Tavera, J.-P. Avouac, D. Remy, J.-M. Nocquet, F. Rolandone, F. Bondoux, G. Gabalda, and S. Bonvalot, 2011. Interseismic coupling and seismic potential along the Central Andes subduction zone, J. Geophys. Res., 116, B12405, doi:10.1029/2010JB008166.
3. Dorbath, L., et al. [1990], Assessment of the size of large and great historical earthquakes in Peru, Bull. Seismol. Soc. Am., 80(3), 551– 576.
4. Dorbath, L., C. Dorbath, E. Jimenez, and L. Rivera, 1991, Seismicity and tectonic deformation in the Eastern Cordillera and the sub-Andean zone of central Peru, Journal of South American Earth Sciences, Vol. 4., No.1/2, 13-24.
5. Mai, P.M., P. Spudich, and J. Boatwright (2005). Hypocenter Locations in Finite-Source Rupture Models, *Bull. Seism.Soc. Am.*, 95, 965-980, doi: 10.1785/0120040111.
6. Perfettini, H., et al. [2010], Aseismic and seismic slip on the Megathrust offshore southern Peru revealed by geodetic strain before and after the Mw8.0, 2007 Pisco earthquake., *Nature*, V. 465, P. 78–81. doi:10.1038/nature09062.
7. Pulido, N., and T. Kubo, 2004, Near-Fault Strong Motion Complexity of the 2000 Tottori Earthquake (Japan) from a Broadband Source Asperity Model, *Tectonophysics*, 390, 177-192.
8. Quispe G., 2010, Preliminary analysis for evaluation of local site effects in Lima city, Peru from strong ground motion data by the spectral method, Master Thesis, National Graduate Institute for Policy Studies, Building Research Institute, Japan, 32p.
9. Ripperger, J., and P. M., Mai, 2004, Fast computation of static stress changes on 2D faults from final slip distributions, *Geophys. Res. Lett.*, 31, L18610, doi:10.1029/2004GL020594.
10. Sladen, A., et al. [2010], Source model of the 2007 Mw 8.0 Pisco, Peru earthquake: Implications for seismogenic behavior of subduction megathrusts, J. Geophys. Res., 115, B02405, doi:10.1029/2009JB006429.